Optical properties and bandgap analysis of multilayer sol-gel $Ba_{1-x}Gd_xTiO_3$ thin films for AR coating application

ALA'EDDIN A. SAIF[1,*], YEN CHIN TEH[2]
[1]*Physics department, College of Science, University of Jeddah, Jeddah, Saudi Arabia*
[2]*Unit Process Development Engineer, Infineon Technologies (Kulim) Sdn Bhd. Kedah, Malaysia*

Perovskites are promising materials for being used as an antireflection (AR) coating in conventional solar cells due to their high refractive index and reasonable energy bandgap. In this work, perovskite-structured $Ba_{1-x}Gd_xTiO_3$ thin films at different Gd^{3+} contents and thicknesses have been prepared via the sol-gel technique and tested using UV-Vis spectroscopy to investigate their possibility of being used as an AR coating. The results show relatively high transmittance and low reflectance for all films in the range of wavelengths from 400 nm to 850 nm; the variation of transmittance and reflectance with Gd^{3+} content and film thickness is attributed to the scattering of light with the microstructure. In the range of wavelengths from 200 nm to 400 nm, high absorbance is observed that is gradually reduced with the Gd^{3+} ratio and increases with film thickness, which is attributed to the grain size effect. The optical bandgap energy for films shows an increase from 3.94 eV to 4.14 eV as the Gd^{3+} content increases from 0.05 to 0.3, while it decreases from 3.84 eV to 3.77 eV with the film thickness, which is also correlated to the grain size variation. The relatively high energy bandgap, high transmittance, low reflectance, and low absorption for $Ba_{1-x}Gd_xTiO_3$ thin films in the wavelength range of 400-850 nm make them potential candidates for AR coating in conventional solar cells. The high absorption in the wavelength range of 200 nm to 400 nm leads to conclude using a top layer of these films is suitable for UV absorption in addition to their role as an antireflection layer for visible wavelengths.

(Received March 5, 2023; accepted April 10, 2024)

Keywords: $Ba_{1-x}Gd_xTiO_3$, Transmittance, Reflectance, Optical bandgap AR coating

1. Introduction

Ferroelectric barium titanate ($BaTiO_3$) has been extensively studied for many applications, such as dynamic random access (DRAM) ferroelectric memories, multilayered ceramic capacitors, and electro-optic devices, due to its excellent dielectric, optical, and ferroelectric characteristics [1-3]. $BaTiO_3$ thin films are also characterized by long-range UV-Vis transparency and a comparably high index of refraction [4-6]. These properties are similar for many antireflection coating oxide materials such as ZrO_2 and TiO_2 [7, 8]. Therefore, ferroelectric $BaTiO_3$ could be a promising candidate for AR coating for the solar cells to increase the absorption of photons by reducing the reflection of incident light onto solar cells, increasing the short circuit current (J_{sc}); as a result, increasing the efficiency of solar cells [9]. The advantage of using $BaTiO_3$ as AR coating material is due to the variety of techniques of preparation, which are mostly low in cost.

This work proposes introducing the transition Gd^{3+} ions as a dopant for Ba; the selection is based on its good optical properties in oxide form, making Gd_2O_3 a good candidate for many nanophotonics and optoelectronics applications [10]. In Gd^{3+} doped $BaTiO_3$, the Gd^{3+} ions substitute whether on Ba^{2+} or Ti^{3+} site in its lattice structure depends on the doping percentage, which directly alters the electrical and optical properties of the material [11]. A study by Fasasi *et al.* [12] reports that Gd^{3+} doped $BaTiO_3$ shows high transmittance within the visible range, and the cut-off wavelength is localized between UV and visible wavelengths. Besides, it offers a high refractive index value, which makes it a suitable candidate for AR coating for solar cell applications.

Minimal studies in the literature report the optical characteristics of Gd^{3+} doped $BaTiO_3$. Our previous work reports the impact of annealing temperature on the optical bandgap energy, showing a decrement trend with the annealing temperature [13]. The current work aims to investigate the effect of doping concentration and film thickness on the optical properties of Gd^{3+} doped $BaTiO_3$ in addition to the optical bandgap energy to be used as an antireflection coating. Thus, films of the $Ba_{1-x}Gd_xTiO_3$ formula at different Gd^{3+} molar ratios are fabricated at different thicknesses via a sol-gel approach. The optical properties of the films are studied using UV-Vis spectrophotometry and correlated to the film structure. Besides, the films' optical bandgap energy value is evaluated with the aid of the transmittance spectrum.

2. Methodology

$Ba_{1-x}Gd_xTiO_3$ solutions at different molar ratios, namely at x = 0, 0.05, 0.1, 0.15, 0.2, 0.25, 0.3, have been

synthesized. Where barium and gadolinium in acetate composition and titanium (IV) isopropoxide are used as the raw materials. The solutions synthesis process uses the procedure described in previous work [13]. Two sets of samples at different molar concentrations and thicknesses are fabricated by depositing the solutions on pre-cleaned UV-grade fused silica (JGS1) substrates due to high transparency over a wide range of wavelengths. The fabrication process for all films is performed similarly as described in previous work and annealed at 800 °C for one hour in the atmosphere [14]. The first set is named based on the molar ratio for the barium to gadolinium as Ba:Gd, while the second set is fabricated for the Gd^{3+} molar ratio of 0.05 and named based on the film thickness.

Due to the amorphous structure of silica substrate, the perovskite structure for $Ba_{1-x}Gd_xTiO_3$ films is characterized on SiO_2/Si substrate by X-ray diffractometer (XRD6000, Shimadzu) using Cu-ka radiation source (λ = 1.5406 Å). For thickness measurement, the films are partially etched to create a step profile; then, this step is used to measure the film thickness using stylus profilometry. It is found that the average film thickness for the second set of samples is 269.57 nm, 332.96 nm, 416.89 nm, and 502.15 nm. The transmittance, absorbance, and reflectance spectra for $Ba_{1-x}Gd_xTiO_3$ thin films on silica substrates are measured at a normal angle, in the range of wavelengths from 200 nm to 800 nm at room temperature using an Ultraviolet-Visible Spectrophotometer (UV-Vis, Perkin Elmer Lambda 950).

3. Results and discussion

3.1. Structure analysis

To confirm the perovskite structure of $Ba_{1-x}Gd_xTiO_3$ films in this study, the XRD patterns of the films at different molar ratios and an annealing temperature of 800 ^oC are presented in Fig. 1. A slight shifting for peaks toward a higher angle, except for (100) peak, with the increase of Gd^{3+} content as compared with the non-doped sample. This indicates that the smaller ionic radius Gd^{3+} ions (0.94 Å) substitute for larger ionic radius Ba^{2+} ions (1.34 Å); as a result, a smaller crystal would be obtained [14-15]. To confirm the reduction in crystallite size, the lattice parameters are determined using Highscore Plus software and summarised in Table 1. It is noticed that *a* and *c* lattice parameters reduce; thus, the lattice volume with the increases of Gd^{3+} content. Moreover, the ratio of c/a is noticed to be greater than 1 for all samples confirming the tetragonality of the films.

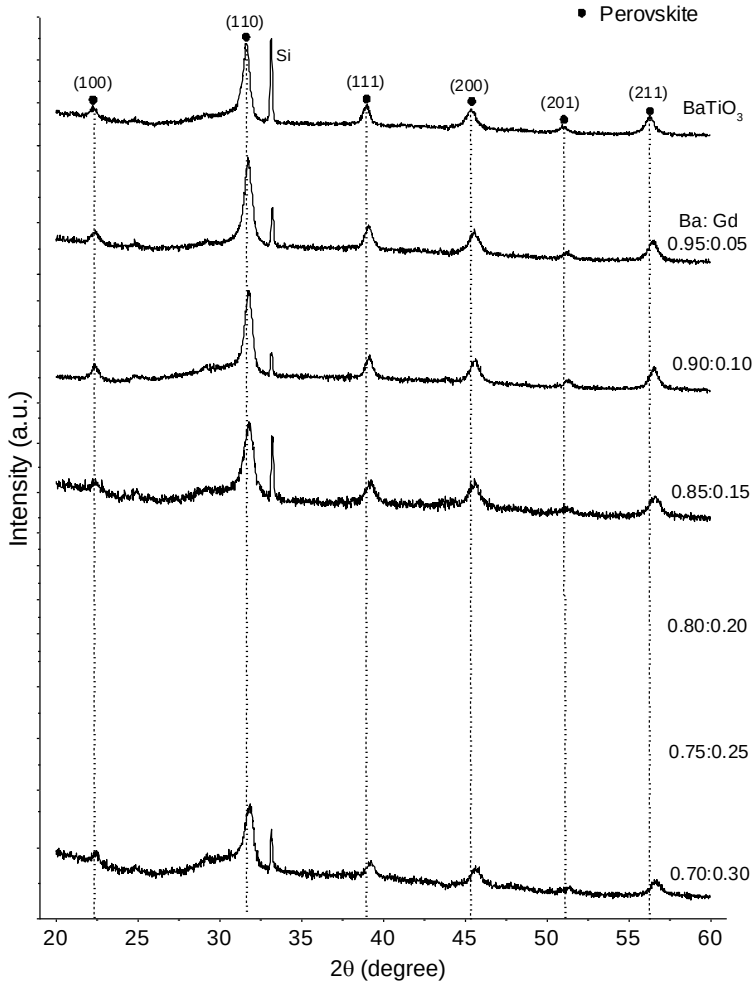

Fig. 1. XRD patterns of $Ba_{1-x}Gd_xTiO_3$ films at different Gd^{3+} content annealed at 800 ^oC

Table 1. Lattice parameters for $Ba_{1-x}Gd_xTiO_3$ films

Sample	Lattice constant, *a* (Å)	Lattice constant, *c* (Å)	Tetragonality c/a ratio	Lattice Volume, *V* (Å^3)
$BaTiO_3$	3.994 ±0.005	4.029 ±0.010	1.00876	64.28
0.95:0.05	3.981 ±0.006	4.032 ±0.013	1.01281	63.90
0.90:0.10	3.981 ±0.005	4.026 ±0.012	1.01130	63.81
0.85:0.15	3.979 ±0.004	4.024 ±0.013	1.01130	63.70
0.80:0.20	3.975 ±0.007	4.012 ±0.016	1.00930	63.41
0.75:0.25	3.969 ±0.004	3.998 ±0.012	1.00730	62.99
0.70:0.30	3.967 ±0.003	3.991 ±0.015	1.00605	62.82

3.2. UV-Vis spectrophotometry analysis

The transmittance spectrum of $Ba_{1-x}Gd_xTiO_3$ thin films at different x values and film thicknesses of the Gd^{3+} molar ratio of 0.05 is shown in Fig. 2. It can be observed that all films reveal transparency greater than 70% in the range of wavelengths from 400 nm to 850 nm. The transmittance increases from 80% to 93% with the increase of Gd^{3+} content, as illustrated in Fig. 2(a). The high transparency of $Ba_{1-x}Gd_xTiO_3$ thin films within the visible spectrum suggests using it as an antireflection layer to enhance conventional solar cell efficiency. In Fig. 2(b), it can be noticed that the transmittance decreases with the film thickness, which is more obvious in the wavelength region of 400 nm to 500 nm, where above this range of wavelength, the transmittance fluctuates forming interference fringes for the thicker film. A similar trend for the transmittance with film thickness for indium oxide thin films at different thicknesses is observed by Nouadji et al. [16]. Moreover, the transmittance is observed to fall to its minimum value in the wavelength range of 350 nm to 200 nm for all samples. The low transmittance value over this wavelength range shows that the $Ba_{1-x}Gd_xTiO_3$ films tend to respond effectively to UV wavelength, which will be discussed further in the absorption part in the following paragraphs.

The variation of transmission, in the range of wavelengths from 400 nm to 850 nm, with molar ratio and film thickness, is attributed to the scattering of light with the microstructure of the films. As the light incident into polycrystalline films, it suffers several scatterings with microstructure imperfections depending on the film's surface roughness, grain size, and grain boundaries. Thus, the effectiveness of scattering gets higher with the increase in the grain size and surface roughness, thus, reducing the transmittance of light through the films. It is discussed in previous work that the grain size and roughness average are decreased with the increase of Gd^{3+} content [14], which explains the increment of the transmittance with the increase of Gd^{3+} content. Moreover, the grain size and roughness average increased with the film thickness [14], which explains the decrement in the transmittance with the increase of film thickness. A similar reduction in transmittance with film thickness is also observed by Singh et al. [17], Soram et al. [18], and Batra et al. [19].

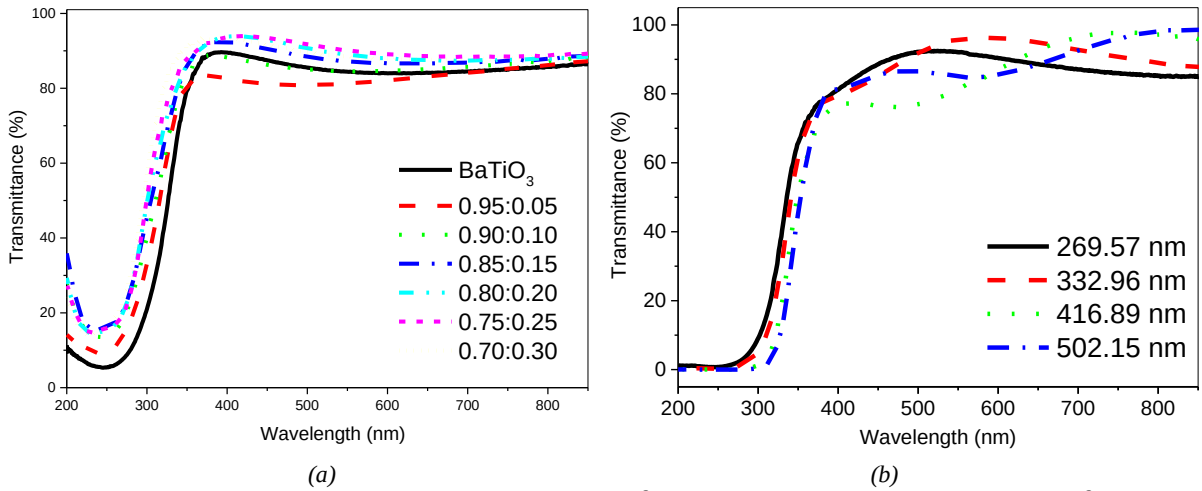

(a) *(b)*

Fig. 2. Transmittance spectra of $Ba_{1-x}Gd_xTiO_3$ films at different (a) Gd^{3+} contents and (b) film thicknesses for the Gd^{3+} molar ratio of 0.05 (color online)

The absorbance and reflectance spectra of $Ba_{1-x}Gd_xTiO_3$ films at different Gd^{3+} contents are illustrated in Fig. 3. In the range of wavelengths from 200 nm to 400 nm, the films reveal relatively high absorbance denoting that more photons are being trapped and absorbed by films. The high absorbance in this wavelength range confirms the UV absorption ability of $Ba_{1-x}Gd_xTiO_3$ films, leading to conclude the possibility of using $Ba_{1-x}Gd_xTiO_3$ as a top layer in a conventional solar cell to absorb solar UV wavelengths. The low absorbance in the wavelength region of 400 nm to 850 nm, in Fig. 3(a), is consistent with the high transparency in the same wavelength range shown in Fig. 2(a). It can be noticed from Fig. 3(a) that the highest absorbance is obtained for a 0.95:0.05 ratio, and it gradually decreases with Gd^{3+} content. This decrement is correlated to the decrease in grain size with the Gd^{3+} ratio. Besides, a notable shift in absorbance threshold towards shorter wavelength with Gd^{3+} content. This shifting results from grain size reduction due to the ionic substitution of relatively smaller Gd^{3+} ions on the Ba^{2+} site.

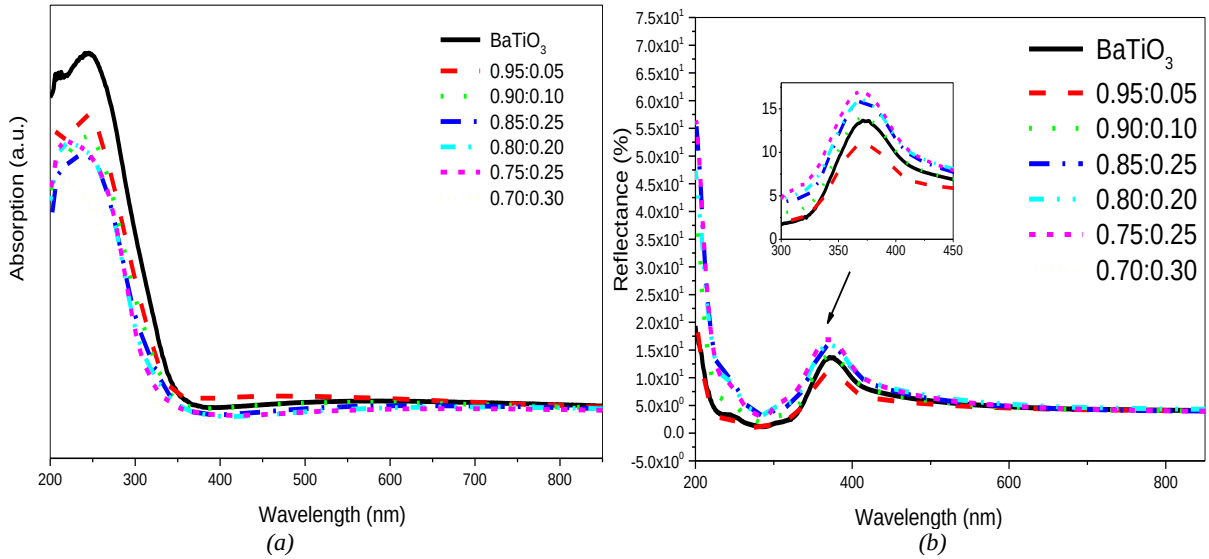

Fig. 3. (a) Absorbance and (b) reflectance spectra for $Ba_xGd_{1-x}TiO_3$ film at different Gd^{3+} contents (color online)

On the other hand, the reflectance spectrum shown in Fig. 3(b) illustrates relatively low reflectance for all $Ba_{1-x}Gd_xTiO_3$ films within the visible region, which supports the possibility of using this material as an AR coating for conventional solar cells. In the range of wavelengths from 300 nm to 450 nm, a peak in the reflectance spectrum is observed, where its intensity increases gradually as Gd^{3+} content increases up to 17%. According to Cui *et al.* [20], the light scattering within polycrystalline materials is directly proportional to the surface roughness and grain boundaries. It is reported in earlier work that the grain size decreases with Gd^{3+} content, leading to an increase in grain boundary areas [14]; as a result, more light is scattered. From Fig. 3(b), the sample with a ratio of 0.95:0.05 has a minimum reflectance of 10% compared with the other ratios.

Fig. 4 shows the absorbance and reflectance spectra for $Ba_{1-x}Gd_xTiO_3$ films of x = 0.05 molar ratio with different film thicknesses. It is noted in Fig. 4(a) that the absorption in the range of wavelengths from 200 nm to 350 nm increases with the film thickness. This trend of absorbance with the film thickness could be explained based on the Beer-Lambert law, which is given by [21]

$$I_T = I_0 exp^{-\alpha d} \quad (1)$$

where I_0 is the incident light intensity, I_T is the transmitted light intensity, α is the coefficient of absorption, and d is the film thickness.

From this relation, one can notice that less transmitted light intensity is obtained for thicker film, which indicates that higher light would be absorbed. This variation in absorption with film thickness can also be attributed to the increment of grain size. The grain size increases as the film becomes denser, leading to smaller grain boundary areas [14]. As a result, more photons will be trapped, and higher absorbance will be obtained. From Fig. 4(b), it can be seen that the reflectance peak intensity increases with film thickness, where the film of a thickness of 502.15 nm exhibits the highest peak intensity of 19%. This increment in reflectance peak intensity is attributed to the surface roughness resulting from larger grain formation of a thicker film.

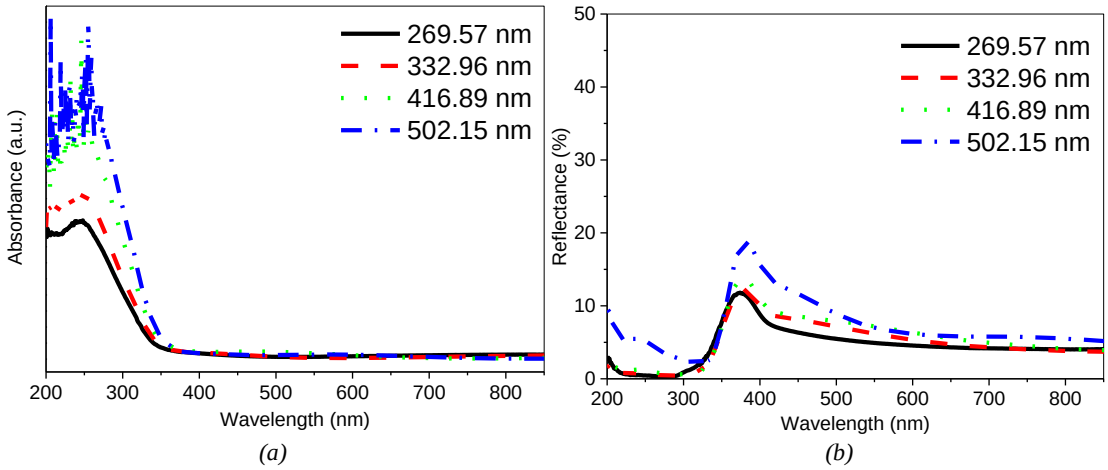

Fig. 4. (a) Absorbance and (b) reflectance spectra for $Ba_{0.95}Gd_{0.05}TiO_3$ films at different thicknesses (color online)

3.3. Optical bandgap analysis

Evaluating the optical bandgap energy value is an important step to realizing the electron transition mechanism between valence and conduction bands in a material corresponding to light absorption [22]. The optical bandgap energy for $Ba_{1-x}Gd_xTiO_3$ films can be estimated using the Tauc relation that is given by [23]

$$h\nu\alpha(E) = B(h\nu - E_g)^{\frac{1}{2}} \quad (2)$$

where $h\nu$ is the photon energy, E_g is the optical bandgap energy, and B is a constant. The coefficient of absorption (α) can be evaluated depending on the transmittance spectra using the following formula [24]

$$\alpha(\lambda) = \frac{1}{d} ln \frac{1}{T} \quad (3)$$

where d is the film thickness, and T is the transmittance.

Fig. 5 illustrates the Tauc plot of $(\alpha h\nu)^2$ versus photon energy for $Ba_{1-x}Gd_xTiO_3$ films at different Gd^{3+} contents and film thicknesses of the Gd^{3+} molar ratio of 0.05. The value of the optical bandgap energy of the films can be estimated by extrapolating the linear part of the plot (not shown in the plot due to overlapping) towards the intercept where the y-axis is zero. Thus, the x-axis intercept would be the value of the corresponding bandgap energy. The value of optical bandgap energy for all samples is given in the legend of the figure. The linear behavior of the plots confirms the direct bandgap of the $Ba_{1-x}Gd_xTiO_3$ films, which is also comparable to other works on $BaTiO_3$-based thin films [25].

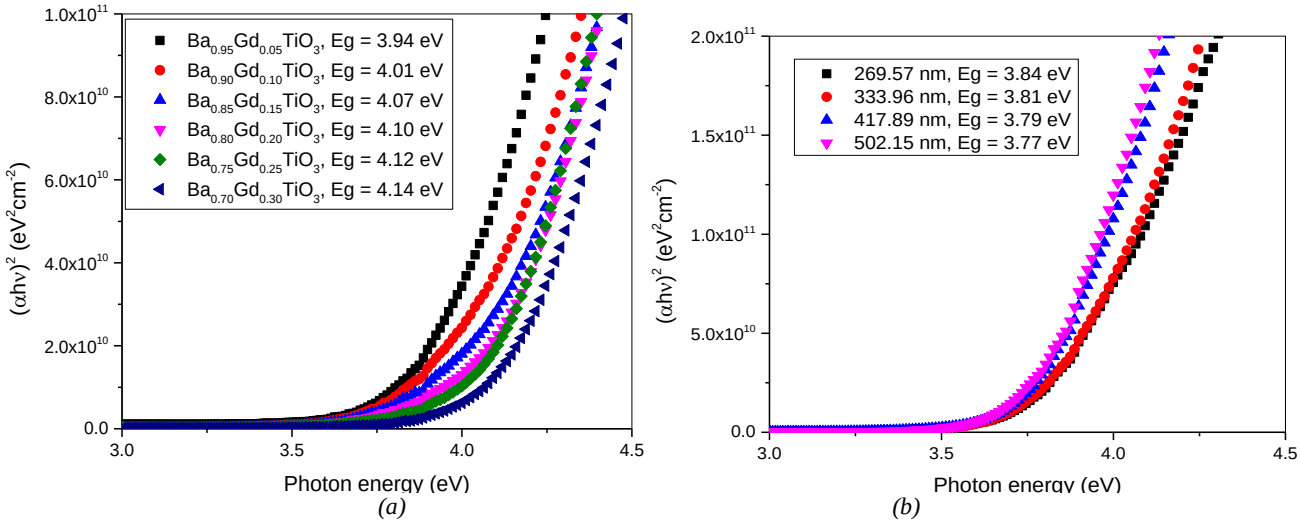

Fig. 5. The Tauc plot fitting of $Ba_xGd_{1-x}TiO_3$ films at different (a) Gd^{3+} contents and (b) film thicknesses for the Gd^{3+} molar ratio of 0.05 (color online)

The estimated optical bandgap energy of $Ba_{1-x}Gd_xTiO_3$ thin films is plotted as a function of Gd^{3+} content and film thickness for the Gd^{3+} molar ratio of 0.05, as shown in Fig. 6. It can be seen that the optical bandgap energy value increases from 3.94 eV to 4.14 eV as the Gd^{3+} content increases from 0 to 0.3. At the same time, it decreases from 3.84 eV to 3.77 eV as the film thickness increases from 269.57 nm to 502.15 nm. These optical

bandgap energy values are comparable with the reported values in the literature for $BaTiO_3$-based films [25]. Furthermore, the large value of optical bandgap energy of $Ba_{1-x}Gd_xTiO_3$ films indicates that this material is a good choice for AR coating for conventional solar cells.

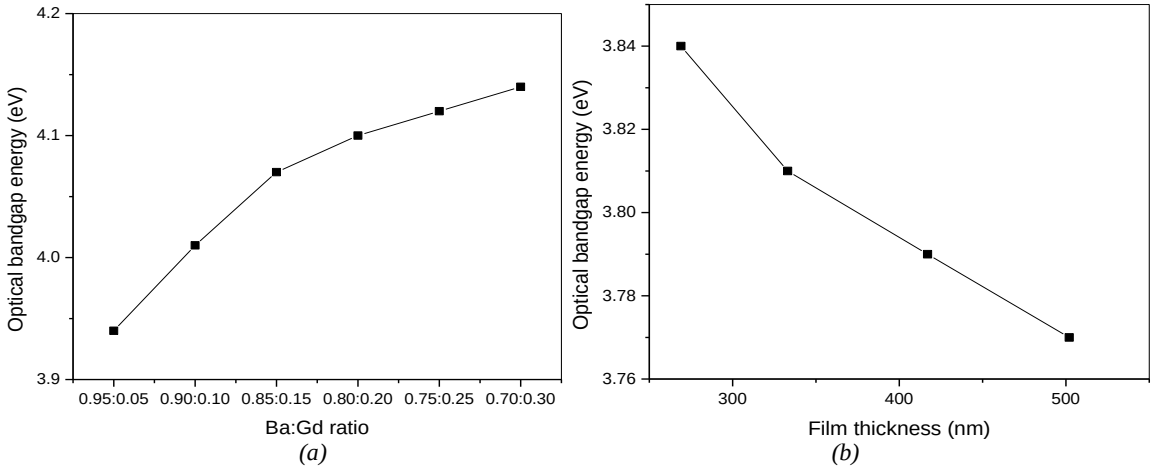

Fig. 6. Variation of optical band gap for $Ba_xGd_{1-x}TiO_3$ films at different (a) Gd^{3+} ratios and (b) film thickness at the Gd^{3+} molar ratio of 0.05

The increment in optical bandgap energy with the increase in Gd^{3+} content in $Ba_{1-x}Gd_xTiO_3$ and the decrement in its value with the film thickness can be attributed to the grain size effect, where the grain size decreases with Gd^{3+} content and increases with film thickness. According to Koole et al. [26], the electronic structure in a nanoscale crystal is strongly dependent on crystallite size. In films with nanostructure, the reduction in unit cell volume and atomic separation result from residual compressive stress, creating large grain boundary areas that subsequently modify the optical bandgap energy of the material. Thus, the reduction in grain size with Gd^{3+} content leads to a large area of grain boundaries, which could result in a potential barrier that gives rise to an increase in the energy difference between the edge of the bands in the electronic structure; thus, bandgap shifts to higher energy [15]. The decrement in optical bandgap energy with film thickness can be explained using the same theory.

4. Conclusion

The effect of molar ratio and film thickness of $Ba_{1-x}Gd_xTiO_3$ thin films fabricated using the sol-gel approach and annealed at 800 °C is investigated. The transmittance, absorbance, and reflectance spectra have been extracted using a UV-Vis Spectrophotometer. It is found that the transmittance for all films is greater than 70% in the range of wavelengths from 400 nm to 850 nm, whereas it shows an increment trend with Gd^{3+} content and a decrement trend with the film thickness. A relatively low reflectance with a peak in the 400-850 nm wavelength region is observed. The transmittance and reflectance variations are correlated to the light scattering with the microstructure. The optical bandgap energy of the films is evaluated based on the transmittance spectrum with the aid of the Tauc relation. The estimated value of the optical bandgap energy increases from 3.94 eV to 4.14 eV with the increase of Gd^{3+} content and decreases from 3.84 eV to 3.77 eV as the film thickness increases. The relatively high energy bandgap, high transmittance, and low reflectance for $Ba_{1-x}Gd_xTiO_3$ thin films make them potential candidates for AR coating for conventional solar cells for the wavelength range of 400-850 nm. Moreover, the absorbance spectrum in the wavelength region of 200-400 nm shows a high value, which reduces with Gd^{3+} content and increases with film thickness. The absorption variation is attributed to the grain size effect. The high absorption for $Ba_{1-x}Gd_xTiO_3$ thin films within the UV range leads to the conclusion that these films are possible to be used as a top layer in conventional solar cells to absorb solar UV wavelength besides its function as an antireflection layer for visible wavelengths.

Acknowledgments

Both authors would like to acknowledge the School of Microelectronics at the University Malaysia Perlis for using their laboratories.

References

[1] Y. Hao, Z. Feng, S. Banerjee, X. Wang, S. J. L. Billinge, J. Wang, L. Li, Journal of Materials Chemistry C **9**(15), 5267 (2021).
[2] V. N. Reddy, C. B. N. Kadiyala, T. Subbarao, Journal of Ovonic Research **12**, 185 (2016).
[3] A. Debnath, V. Srivastava, S. S. Sunny, Appl. Phys. A **126**, 36 (2020).
[4] L. V. Maneeshya, V. S. Anitha, P. V. Thomas, K. Joy, Journal of Materials

Science: Materials in Electronics **26**, 2947 (2015).
[5] V. Kaushik, V. Kumar, D. Kumar, R. Kumar, V. Singh, M. Kumar, S. K. Sharma, Applied Surface Science Advances **16**, 100418 (2023).
[6] A. A. Saif, Y. C. Teh, P. Poopalan, Matéria **28** (3), 2023 (2023).
[7] N. Nosidlak, J. Jaglarz, A. Vallati, P. Dulian, M. Jurzecka-Szymacha, S. Gierałtowska, A. Seweryn, Ł. Wachnicki, B. S. Witkowski, M. Godlewski, Coatings **13**, 1872 (2023).
[8] A. Singh, R. Ghosh, P. Agarwal, Journal of Materials Science: Materials in Electronics **34**, 1235 (2023).
[9] N. N. Hamdan, N. Yusof, M. Z. Mohd Yusoff, Trends in Science **20**, 7337 (2024).
[10] Y. A. Kuznetsova, A. F. Zatsepin, IOP Conference Series: Journal of Physics **917**, 062001 (2017).
[11] Y. Han-Sol, Sh. Jae-Hyeon, K. Yong-Seon, K. Su-Yeon, Sh. So-Young, P. Kwon-Jin, Y. Chun-Yeol, J. Dae-Yong, Ch. Nam-Hee, Bulletin of Materials Science **44**, 241 (2021).
[12] A. Y. Fasasi, B. D. Ngom, J. B. Kana-Kana, R. Bucher, M. Maaza, C. Theron, U. Buttner, Journal of Physics and Chemistry of Solids **70**, 1322 (2009).
[13] Y. C. Teh, A. A. Saif, Journal of Alloys and Compounds **703**, 407 (2017).
[14] A. A. Saif, Y. Ch. Teh, Physica B: Condensed Matter **612**, 412824 (2021).
[15] M. T. Rahman, C. V. Ramana, Ceramics International **40**, 14533 (2014).
[16] R. Nouadji, A. Attaf, A. Derbali, A. Bouhdjer, H. Saidi, M. S. Aida, F. Zeribi, O. Benkhetta, R. Messemeche, M. Nouadji, N. Attaf, Main Group Chemistry **20**(4), 513 (2021).
[17] S. Bobby Singh, H. B. Sharma, H. N. K. Sarma, S. Phanjoubam, Physica B: Condensed Matter **403**, 2678 (2008).
[18] B. S. Soram, B. S. Ngangom, H. B. Sharma, Thin Solid Films **524**, 57 (2012).
[19] V. Batra, S. Kotru, M. Varagas, C. V. Ramana, Optical Materials **49**, 123 (2015).
[20] H. Cui, V. Teixeira, L. Meng, R. Martins, E. Fortunato, Vacuum **82**, 1507 (2008).
[21] A. Mendoza-Galván, J. G. Méndez-Lara, R. A. Mauricio-Sánchez, K. Järrendahl, H. Arwin, Optics Letters **46**(4), 872 (2021).
[22] K. N. Manjunatha, S. Paul, Applied Surface Science **352**, 10 (2015).
[23] H. A. Gatea, Journal of Materials Science: Materials in Electronics **34**, 479 (2023)
[24] M. Junaid, Kh.M. Batoo, S.G. Hussain, S. Hussain, Results in Chemistry **6**, 101177 (2023).
[25] A. Gaur, N. Sharma, International Journal of Engineering, Mathematical and Physical Sciences **7**(12), 1 (2013).
[26] R. Koole, E. Groeneveld, D. Vanmaekelbergh, A. Meijerink, C. de Mello Donegá, Size Effects on Semiconductor Nanoparticles, edited by C. de Mello Donegá, Springer, Berlin, Heidelberg, 2014.

*Corresponding author: aasaif@uj.edu.sa